Journal of Hydroscience and Hydraulic Engineering
Vol. 29, No.1 May, 2011, 15-32

NUMERICAL AND EXPERIMENTAL ANALYSIS ON DEPOSITION PROCESS OF DEBRIS FLOW WITH DRIFTWOOD ON THE FAN

By

Badri Bhakta Shrestha

Disaster Prevention Research Institute, Kyoto University, Gokasho Uji, Kyoto, Japan

Hajime Nakagawa

Disaster Prevention Research Institute, Kyoto University, Gokasho Uji, Kyoto, Japan

Kenji Kawaike

Disaster Prevention Research Institute, Kyoto University, Gokasho Uji, Kyoto, Japan

Yasuyuki Baba

Disaster Prevention Research Institute, Kyoto University, Gokasho Uji, Kyoto, Japan

and

Hao Zhang

Disaster Prevention Research Institute, Kyoto University, Gokasho Uji, Kyoto, Japan

SYNOPSIS

The deposition process of debris flows with driftwood on the fan was investigated through the numerical model and laboratory experiments. A two-dimensional numerical model was developed for computing the characteristics of debris flow with driftwood, which can simulate all the stages of debris flow including initiation, transportation and deposition stages. A numerical model was developed with an interacting combination of Eulerian expression of the debris flow and Lagrangian expression of the driftwood. The calculated results of the shapes and thicknesses of a debris flow fan and the positions and the rotational angles of deposited driftwood in a debris flow fan were consistent with the experimental results. The effects of check dams on the formation of debris flow fan were also investigated.

INTRODUCTION

Debris flow is generally described as gravity flow of a mixture of soil, rocks and water (1). Debris flow is often generated by the erosion of steep debris beds in gullies. When the debris flow reaches a gentle basin from the steep channel, it spreads out, reduces its momentum and then stops after reaching a flatter area. Sediment deposits

and leaves mud fluid or clear water flow downstream. This process gradually creates a debris flow fan (1), (2). Many settlement areas are located at the foot of mountains, where debris flow spreads and deposits. As result disastrous damage and sometimes considerable loss of life and property may occur. Thus, it is necessary to study on deposition of debris flow with driftwood on the fan to establish "soft" countermeasures for debris flow hazards.

Many researchers such as Takahashi et al. (1), Tsai (2), Shieh et al. (3), Ghilardi et al. (4), Rickenmann et al. (5) and others have proposed numerical model to compute the deposition of debris flows on the fan with considering debris flow as sediment water mixture only. However, in recent years debris flow flows with driftwood due to heavy downpours over mountainous rivers (6). Based on the observations of past experiences, it is clear that the most serious damage has occurred when the debris flow flows with driftwood. Thus, an examination of the deposition of debris flows with driftwood on the fan is very important for the prediction of hazards zone and to establish the soft countermeasures. An investigation into the scattering and deposition processes of driftwood in a debris flow fan is also necessary. Previous researchers have not focused on computing the deposition of debris flows with driftwood on the fan. On the other hand, few researchers have investigated the behavior of driftwood only with clear water flow case (7), (8). Furthermore, most studies have focused on assessing specific stages of debris flow. Nevertheless, there is a pressing need for more advanced models that can smoothly seamlessly all stages of movement initiation, transportation and deposition of debris flow with driftwood and thereby improve forecasting ability.

Numerical analysis and experimental studies are carried out to investigate the deposition of debris flows with driftwood on the fan. A two-dimensional integrated numerical model is developed for computing the characteristics of debris flow with driftwood, which can simulate all the stages of debris flow initiation, transportation and deposition stages. A numerical simulation model is developed with an interacting combination of Eulerian expression of the debris flow and Lagrangian expression of the driftwood. A capturing model of debris flow with driftwood by open type check dams is also incorporated into an integrated numerical model. The driftwood deposition process of investigating the positions and the rotational angles of deposited driftwood in a debris flow fan is also incorporated into an integrated numerical model. The effects of driftwood and check dams on debris flow fan formation are also investigated numerically and experimentally.

DEBRIS FLOW WITH DRIFTWOOD MODEL

Basic equations of debris flow motion

The depth-wise averaged two-dimensional momentum equations of debris flow for the x–wise (down valley) and y-wise (lateral) directions are described as follows:

$$\frac{\partial M}{\partial t}+\beta\frac{\partial(uM)}{\partial x}+\beta\frac{\partial(vM)}{\partial y}=gh\sin\theta_{bx0}-gh\cos\theta_{bx0}\frac{\partial(z_b+h)}{\partial x}-\frac{\tau_{bx}}{\rho_T}+\frac{\tau_{sx}}{\rho_T} \tag{1}$$

$$\frac{\partial N}{\partial t}+\beta\frac{\partial(uN)}{\partial x}+\beta\frac{\partial(vN)}{\partial y}=gh\sin\theta_{by0}-gh\cos\theta_{by0}\frac{\partial(z_b+h)}{\partial y}-\frac{\tau_{by}}{\rho_T}+\frac{\tau_{sy}}{\rho_T} \tag{2}$$

The continuity equation of the total volume is

$$\frac{\partial h}{\partial t}+\frac{\partial M}{\partial x}+\frac{\partial N}{\partial y}=i_b \tag{3}$$

The continuity equation of the sediment particles fraction is

$$\frac{\partial(Ch)}{\partial t}+\frac{\partial(CM)}{\partial x}+\frac{\partial(CN)}{\partial y}=i_b C_* \tag{4}$$

The equation for the change of bed surface elevation is

$$\frac{\partial z_b}{\partial t}+i_b=0 \tag{5}$$

where, $M\ (=uh)$ and $N\ (=vh)$ = the flow discharge per unit width in x and y directions; u and v = the velocity components in x and y directions; h = the flow depth; z_b = the erosion or deposition thickness of the bed measured from the original bed surface elevation; θ_{bx0} and θ_{by0} = the x and y components of the slope of the original bed surface of the flume; i_b = the erosion/deposition velocity; C = the sediment concentration in the flow; C_* = the sediment concentration in the bed; β = the momentum correction factor equal to 1.25 for stony debris flow (1) and to 1.0 for both an immature debris flow and a turbulent flow; g = the acceleration due to gravity; τ_{bx} and τ_{by} = the bottom shear stresses in x and y direction; ρ_T = mixture density ($\rho_T=\sigma C+(1-C)\rho$, σ = density of the sediment particles and ρ = density of the water); and τ_{sx} and τ_{sy} = the shear stresses at the flow surface in x and y directions generated as the reaction of the drag force acting on the driftwood.

The bottom resistance for a two-dimensional flow is described as follows (9). For a fully developed stony debris flow ($C>0.4C_*$);

$$\tau_{bx}=\frac{u}{\sqrt{u^2+v^2}}f(C)(\sigma-\rho)Cgh\cos\theta_x\tan\phi+\rho\frac{1}{8}\frac{(\sigma/\rho)}{\left\{(C_*/C)^{1/3}-1\right\}^2}\left(\frac{d_m}{h}\right)^2 u\sqrt{u^2+v^2} \tag{6}$$

$$\tau_{by}=\frac{v}{\sqrt{u^2+v^2}}f(C)(\sigma-\rho)Cgh\cos\theta_y\tan\phi+\rho\frac{1}{8}\frac{(\sigma/\rho)}{\left\{(C_*/C)^{1/3}-1\right\}^2}\left(\frac{d_m}{h}\right)^2 v\sqrt{u^2+v^2} \tag{7}$$

$$f(C)=\begin{cases}\dfrac{C-C_3}{C_*-C_3} & ;\ C>C_3\\ 0 & ;\ C\le C_3\end{cases} \tag{8}$$

For an immature debris flow ($0.02\le C\le 0.4C_*$);

$$\tau_{bx}=\frac{\rho_T}{0.49}\left(\frac{d_m}{h}\right)^2 u\sqrt{u^2+v^2}\quad ;\quad \tau_{by}=\frac{\rho_T}{0.49}\left(\frac{d_m}{h}\right)^2 v\sqrt{u^2+v^2} \tag{9}$$

For a turbulent flow ($C<0.02$);

$$\tau_{bx}=\frac{\rho g n^2 u\sqrt{u^2+v^2}}{h^{1/3}}\quad ;\quad \tau_{by}=\frac{\rho g n^2 v\sqrt{u^2+v^2}}{h^{1/3}} \tag{10}$$

where, θ_x and θ_y = the x and y components of the slope of the erodible bed surface; d_m = mean diameter of sediment; C_3 = the limitative sediment concentration; and n = the Manning's coefficient. The slopes θ_x and θ_y are different from the original bed surface slopes of the flume θ_{bx0} and θ_{by0}. The slopes θ_x and θ_y change due to the erosion/deposition process.

The shear stresses at the flow surface in x and y directions generated as the reaction of the drag force acting on the driftwood are described as follows:

$$\tau_{sx}=\frac{1}{A}\sum_{k=1}^{N_t}\left\{\frac{1}{2}\rho_T C_{Dx}W_k(u_k-U_k)A_{kx}\right\}\quad ;\quad \tau_{sy}=\frac{1}{A}\sum_{k=1}^{N_t}\left\{\frac{1}{2}\rho_T C_{Dy}W_k(v_k-V_k)A_{ky}\right\} \tag{11}$$

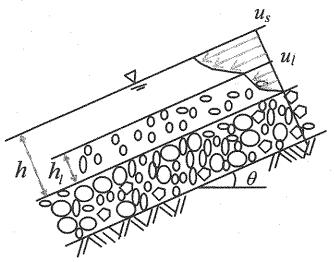

Fig. 1 Schematic illustration of an immature debris flow

where, u_k and v_k = the respective driftwood velocity components in x and y directions; U_k and V_k = the respective local velocity components of the fluid in x and y directions at the position of the centroid of the driftwood; $W_k = \sqrt{(u_k - U_k)^2 + (v_k - V_k)^2}$; A_{kx} and A_{ky} = the respective projected areas of the submerged part of the driftwood in x and y directions; C_{Dx} and C_{Dy} = drag coefficients in x and y directions; $A\ (=\Delta x \Delta y)$ = the area of the flow surface (Δx and Δy = the grid sizes of the finite difference equations); and N_t = the number of total pieces of driftwood in area A.

The flow motion of the piece of driftwood is restricted near the flow surface. Thus, the surface flow velocity components u_s and v_s in x and y directions to compute the driftwood motion are described by integrating the velocity distribution functions given by Takahashi (10) as follows. For a fully developed stony debris flow;

$$u_s = \frac{2}{3d_m}\left[\frac{g\sin\theta_x}{a_i \sin\alpha_i}\left\{C + (1-C)\frac{\rho}{\sigma}\right\}\right]^{1/2}\left\{\left(\frac{C_*}{C}\right)^{1/3} - 1\right\}h^{3/2} \tag{12}$$

$$v_s = \frac{2}{3d_m}\left[\frac{g\sin\theta_y}{a_i \sin\alpha_i}\left\{C + (1-C)\frac{\rho}{\sigma}\right\}\right]^{1/2}\left\{\left(\frac{C_*}{C}\right)^{1/3} - 1\right\}h^{3/2} \tag{13}$$

For an immature debris flow;

$$\frac{u_s}{u_*} = \frac{u_l}{u_*} + + \frac{2}{\kappa}\left\{-\left(1-\frac{h_l}{h}\right)^{1/2}\right\} - \frac{1}{\kappa}\psi \ln\left|\psi\left\{\left(1-\frac{h_l}{h}\right)^{1/2} - \psi\right\} \Big/ \left[(-\psi)\left\{\left(1-\frac{h_l}{h}\right)^{1/2} + \psi\right\}\right]\right| \tag{14}$$

$$\frac{v_s}{v_*} = \frac{v_l}{v_*} + \frac{2}{\kappa}\left\{-\left(1-\frac{h_l}{h}\right)^{1/2}\right\} - \frac{1}{\kappa}\psi \ln\left|\psi\left\{\left(1-\frac{h_l}{h}\right)^{1/2} - \psi\right\} \Big/ \left[(-\psi)\left\{\left(1-\frac{h_l}{h}\right)^{1/2} + \psi\right\}\right]\right| \tag{15}$$

$$\psi = \left(\frac{d_m}{\kappa h}\frac{\varsigma}{\lambda} + 1 - \frac{h_l}{h}\right)^{1/2} \tag{16}$$

where, u_l and v_l = the velocity components of the flow in x and y directions at the thickness of the particle mixture layer in an immature debris flow h_l (Fig. 1); $u_*\ (=\sqrt{gh\sin\theta_x})$ and $v_*\ (=\sqrt{gh\sin\theta_y})$ = the friction velocity components in x and y directions; $\varsigma(=3)$ = constant to describe the mixing length; $\kappa(=0.4)$ = Karman constant; and λ = the linear concentrations. The thickness of the particle mixture layer and the linear concentration are described as follows:

$$\frac{h_l}{h}=\frac{C_\infty}{C_{dl}} \tag{17}$$

$$C_{dl}\approx 0.4C_* \tag{18}$$

$$\lambda=\left\{\left(\frac{C_*}{C}\right)^{1/3}-1\right\}^{-1} \tag{19}$$

and the velocity components u_l and v_l are described as

$$\frac{u_l}{u_*}=\frac{2}{3}\frac{h}{d_m}\frac{1}{\left\{(\sigma/\rho)\lambda^2 a_i\sin\alpha_i+\varsigma^2/\lambda^2\right\}^{1/2}\left\{C_{dl}(\sigma-\rho)/\rho+1\right\}}\eta' \tag{20}$$

$$\frac{v_l}{v_*}=\frac{2}{3}\frac{h}{d_m}\frac{1}{\left\{(\sigma/\rho)\lambda^2 a_i\sin\alpha_i+\varsigma^2/\lambda^2\right\}^{1/2}\left\{C_{dl}(\sigma-\rho)/\rho+1\right\}}\eta' \tag{21}$$

$$\eta'=\left[\eta^{3/2}-\left\{\eta-\left(\frac{\sigma-\rho}{\rho}C_{dl}+1\right)\frac{h_l}{h}\right\}^{3/2}\right] \tag{22}$$

$$\eta=\left(\frac{\sigma-\rho}{\rho}C_{dl}\frac{h_l}{h}+1\right) \tag{23}$$

For a turbulent flow;

$$\frac{u_s}{u_*}=\frac{1}{\kappa}\ln\frac{1+\sqrt{1+\psi_1}}{a_0/R_{*x}+\sqrt{(a_0/R_{*x})^2+\psi_1}}\quad;\quad\frac{v_s}{v_*}=\frac{1}{\kappa}\ln\frac{1+\sqrt{1+\psi_1}}{a_0/R_{*y}+\sqrt{(a_0/R_{*y})^2+\psi_1}} \tag{24}$$

$$\psi_1=\lambda^2(a_i\sin\alpha_i/\kappa^2)(\sigma/\rho)(d_m/h)^2 \tag{25}$$

where, $R_{*x}=u_*h/\upsilon_0$; $R_{*y}=v_*h/\upsilon_0$; $a_0=1/9.025$; $\upsilon_0(=0.01cm^2/\sec)$ = the kinematic viscosity of plain water; a_i = the experimental constant; and α_i = the collisions angle of the particles ($a_i\sin\alpha_i$ =0.02) (10).

The erosion and deposition velocity equations for two dimensional debris flow model given by Takahashi et al. (1) are described as follows: The erosion velocity equation, if $C\le C_\infty$;

$$i_b=\delta_e\frac{C_\infty-C}{C_*-C_\infty}\frac{\sqrt{u^2+v^2}\,h}{d_m} \tag{26}$$

The deposition velocity equation, if $C>C_\infty$;

$$i_b=\delta_d\frac{C_\infty-C}{C_*}\sqrt{u^2+v^2} \tag{27}$$

where, δ_e = the erosion coefficient; δ_d = the deposition coefficient; d_m = the mean diameter of sediment; and C_∞ = the equilibrium sediment concentration described as follows (11), if $\tan\theta_w>0.138$, a stony type debris flow occurs, and

$$C_{\infty} = \frac{\tan\theta_w}{(\sigma/\rho - 1)(\tan\phi - \tan\theta_w)} \tag{28}$$

If $0.03 < \tan\theta_w \leq 0.138$, an immature type debris flow occurs, and

$$C_{\infty} = 6.7\left\{\frac{\tan\theta_w}{(\sigma/\rho - 1)(\tan\phi - \tan\theta_w)}\right\}^2 \tag{29}$$

If $\tan\theta_w \leq 0.03$, a turbulent water flow with bed load transport occurs, and

$$C_{\infty} = \frac{(1+5\tan\theta_w)\tan\theta_w}{\sigma/\rho - 1}\left(1-\alpha_0^2\frac{\tau_{*c}}{\tau_*}\right)\left(1-\alpha_0^2\sqrt{\frac{\tau_{*c}}{\tau_*}}\right) \tag{30}$$

where, ϕ = the internal friction angle of the sediment; θ_w = water surface slope; and

$$\alpha_0^2 = \frac{2\{0.425 - (\sigma/\rho)\tan\theta_w/(\sigma/\rho - 1)\}}{1 - (\sigma/\rho)\tan\theta_w/(\sigma/\rho - 1)} \tag{31}$$

$$\tau_{*c} = 0.04 \times 10^{1.72\tan\theta_w} \tag{32}$$

$$\tau_* = \frac{h\tan\theta_w}{(\sigma/\rho - 1)d_m} \tag{33}$$

where, τ_{*c} = the non-dimensional critical shear stress and τ_* = the non-dimensional shear stress.

The partial differential equations of basic equations of debris flow are obtained from the methods adopted by Nakagawa (12) by using Leap-Frog scheme, in which upwind scheme is adopted in the advection term and implicit scheme is introduced in the friction term.

Basic equations of driftwood motion

It is assumed that the pieces of driftwood are sufficiently dispersed so that collisions between them are infrequent. The flow motion of driftwood is restricted near the flow surface. However, when a debris flow debouches from a canyon mouth at which the slope abruptly becomes flat, its competence to transport sediment markedly decreases and its materials are deposited on the debris fan. The flow motion of driftwood comes into contact with the bed surface after reducing certain flow depth due to debris flow deposition in a fan area. The driftwood stops due to the friction forces generated between the driftwood and the bed surface. By introducing such friction forces, the equations of motion of each piece of driftwood, individually labeled by subscript k are expressed as

$$(m_k + mC_M)\frac{du_k}{dt} = -m_k g\frac{\partial H_k}{\partial x} - \frac{1}{2}\rho_T C_{Dx} W_k (u_k - U_k) A_{kx} \pm F_{fx} \tag{34}$$

$$(m_k + mC_M)\frac{dv_k}{dt} = -m_k g\frac{\partial H_k}{\partial y} - \frac{1}{2}\rho_T C_{Dy} W_k (v_k - V_k) A_{ky} \pm F_{fy} \tag{35}$$

$$\frac{dX_k}{dt} = u_k \quad ; \quad \frac{dY_k}{dt} = v_k \tag{36}$$

where, X_k and Y_k = the position of the centroid of the driftwood; m_k = the mass of the driftwood; m = the mass of the fluid occupied by volume of a piece of driftwood; C_M = the virtual mass coefficient; H_k = the flow level at centroid position of the driftwood; and F_{fx} and F_{fy} = the friction forces in x and y directions. The friction forces are in the opposite direction to the flow motion of driftwood and these forces are described as

$$F_{fx} = \mu_{kx} m_k g \cos(\theta_x)_k \quad ; \quad F_{fy} = \mu_{ky} m_k g \cos(\theta_y)_k \tag{37}$$

and $\partial H_k / \partial x$ and $\partial H_k / \partial y$ are described as

$$-\frac{\partial H_k}{\partial x} = \sin(\theta_{bx0})_k - \cos(\theta_{bx0})_k \frac{\partial (z_b + h)_k}{\partial x} \quad ; \quad -\frac{\partial H_k}{\partial y} = \sin(\theta_{by0})_k - \cos(\theta_{by0})_k \frac{\partial (z_b + h)_k}{\partial y} \tag{38}$$

where, μ_{kx} and μ_{ky} = the kinetic friction coefficients in x and y directions; $(\theta_x)_k$ and $(\theta_y)_k$ = the bed slopes at the position of the centroid of the driftwood in x and y directions; $(\theta_{bx0})_k$ and $(\theta_{by0})_k$ = the x and y components of the slope of the original bed surface at the position of the centroid of the driftwood; and $(z_b + h)_k$ = the flow surface stage $(z_b + h)$ at the position of the centroid of the driftwood. The projected areas A_{kx} and A_{ky} of the submerged part of the driftwood are described as follows:

$$A_{kx} = h_w L_d |\sin \theta_k| \quad ; \quad A_{ky} = h_w L_d |\cos \theta_k| \tag{39}$$

and,

$$A_{kx} = r^2 (\pi - \alpha_1 + \sin \alpha_1 \cos \alpha_1); \quad \text{when} \quad \theta_k = 0 \tag{40}$$

$$A_{ky} = r^2 (\pi - \alpha_1 + \sin \alpha_1 \cos \alpha_1); \quad \text{when} \quad \theta_k = \pi / 2 \tag{41}$$

$$h_w = r(1 + \cos \alpha_1) \tag{42}$$

where, θ_k = the rotational angle of the piece of driftwood; r = the radius of driftwood; L_d = the length of the driftwood piece; h_w = the depth of submerged part of driftwood in the fluid; and α_1 = angle as shown in Fig. 2, which can be determined by equating the weight of driftwood pieces and the weight of fluid occupied by the volume of a piece of driftwood as follows:

$$\rho_d \pi r^2 L_d g = \rho_T r^2 (\pi - \alpha_1 + \sin \alpha_1 \cos \alpha_1) g L_d \tag{43}$$

The rotational motion around the axis of the centroid of the driftwood is described by evaluating the moment N_0 produced by the hydrodynamic force acting on the driftwood. On the supposition that the driftwood can be divided into two pieces at the centroid 'c' and that the drag force acts on both centroids, 'a' and 'b', of these pieces as shown in Fig. 3, the rotational motion of the driftwood is described as follows (7):

$$Id^2\theta_k / dt^2 = \sum N_0 = (L_d / 4)\{(f_{xa} - f_{xb}) \sin \theta_k - (f_{ya} - f_{yb}) \cos \theta_k\} \tag{44}$$

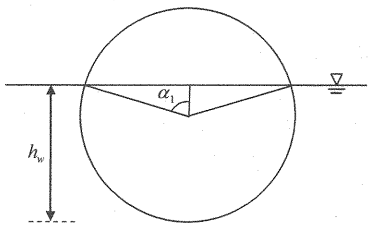

Fig. 2 Definition sketch of angle α_1

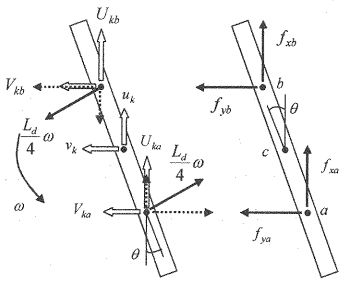

Fig. 3 Definition sketch of the rotational angle of pieces of driftwood

where,

$$f_{xa} = (1/2)\rho_T C_{Dx}\sqrt{(U_{ka}-u_k-u_{rka})^2+(V_{ka}-v_k-v_{rka})^2}\,(U_{ka}-u_k-u_{rka})(A_{kx}/2) \tag{45}$$

$$f_{ya} = (1/2)\rho_T C_{Dy}\sqrt{(U_{ka}-u_k-u_{rka})^2+(V_{ka}-v_k-v_{rka})^2}\,(V_{ka}-v_k-v_{rka})(A_{ky}/2) \tag{46}$$

$$f_{xb} = (1/2)\rho_T C_{Dx}\sqrt{(U_{kb}-u_k-u_{rkb})^2+(V_{kb}-v_k-v_{rkb})^2}\,(U_{kb}-u_k-u_{rkb})(A_{kx}/2) \tag{47}$$

$$f_{yb} = (1/2)\rho_T C_{Dy}\sqrt{(U_{kb}-u_k-u_{rkb})^2+(V_{kb}-v_k-v_{rkb})^2}\,(V_{kb}-v_k-v_{rkb})(A_{ky}/2) \tag{48}$$

$$u_{rka} = (L_d/4)(d\theta_k/dt)\sin\theta_k \quad ; \quad v_{rka} = -(L_d/4)(d\theta_k/dt)\cos\theta_k \tag{49}$$

$$u_{rkb} = -(L_d/4)(d\theta_k/dt)\sin\theta_k \quad ; \quad v_{rkb} = (L_d/4)(d\theta_k/dt)\cos\theta_k \tag{50}$$

where, I = the moment of inertia around the centroid 'c', which is written as $I = m_k(r^2/4 + L_d{}^2/12)$. The rotational motion of the driftwood is also supposed to be restricted on the flow surface and the rotation on the vertical plane is not considered. For the driftwood motion, the space-centered and the time-forward differencing approximation proposed by Nakagawa et al. (13) is adopted.

FLUCTUATION OF POSITION AND ROTATIONAL ANGLE OF DRIFTWOOD

Fluctuation of position of driftwood

The position and the rotational angle of the driftwood can be evaluated deterministically by integrating Eqs. 36 and 44, respectively, but they fluctuate due to the collision of driftwood with boulders and disturbances on the flow surface during the collision of sediment particles. These fluctuation components ΔX_k and ΔY_k are described as (6)

$$\Delta X_k = \sqrt{4K_x(2\Delta t)}\,erf^{-1}(\alpha') \quad ; \quad \Delta Y_k = \sqrt{4K_y(2\Delta t)}\,erf^{-1}(\beta') \tag{51}$$

where, K_x and K_y = the longitudinal and transverse diffusion coefficients; α' and β' = random variables uniformly distributed in the range (0,1); and erf^{-1} = the inverse of error function, erf, given by

$$\left.\begin{aligned} erf(s) &= \left\{1-\Phi(\sqrt{2}s)\right\} = \left(1/\sqrt{\pi}\right)\int_s^{\infty}\exp(-\varepsilon^2)d\varepsilon \\ \Phi(s) &= \left(1/\sqrt{2\pi}\right)\int_{-\infty}^{s}\exp(-\varepsilon^2/2)d\varepsilon \end{aligned}\right\} \tag{52}$$

For the diffusion coefficients of the driftwood, the relations $K_x/u_*h = 0.649$ and $K_y/u_*h = 0.343$, are used as Shrestha et al. (6). The driftwood position is estimated by adding the fluctuation value to the value obtained from the equations of motion deterministically as

$$X_k^{n+3} = X_k^{n+1} + u_k^{n+2}(2\Delta t) + \sqrt{4K_x(2\Delta t)}erf^{-1}(\alpha') \tag{53}$$

$$Y_k^{n+3} = Y_k^{n+1} + v_k^{n+2}(2\Delta t) + \sqrt{4K_y(2\Delta t)}erf^{-1}(\beta') \tag{54}$$

Fluctuation of rotational angle of driftwood

The mean value of the angular velocities is approximately zero, $\overline{\omega} \approx 0$ and the standard deviation of the rotational motion of the driftwood, σ_w, is described to the Froude number, Fr, as $\sigma_w = 25.61Fr$ (6). The rotational angle of the driftwood is evaluated by considering the fluctuation component as follows:

$$d\theta_k/dt = \omega_d + \omega_p \tag{55}$$

$$\theta_k^{n+3} = \theta_k^{n+1} + 2\Delta t(\omega_d + \omega_p) \tag{56}$$

where, ω_d = the angular velocity of the piece of driftwood obtained deterministically and ω_p = the fluctuation of the angular velocity of the driftwood evaluated stochastically. Assuming that the rotational angular velocity of the fluctuating component of a piece of driftwood follows a normal distribution, its distribution function, Φ, is given by

$$\Phi(\gamma) = \frac{1}{\sqrt{2\pi}}\int_{-\infty}^{\gamma}\exp(-\varepsilon^2/2)d\varepsilon \tag{57}$$

where, $\gamma = (\omega_p - \overline{\omega})/\sigma_w$ is obtained from the inverse function, Φ^{-1}, for uniformly distributed random numbers within (0,1); $\overline{\omega}$ and σ_w = the mean and standard deviation of angular velocity of driftwood. After γ is obtained, ω_p is estimated from $\omega_p = \gamma\sigma_w + \overline{\omega}$.

LABORATORY FLUME EXPERIMENTS

A flume channel 2m long, 60cm wide and 20cm deep was connected to the downstream end of 5m long, 10cm wide and 13cm deep flume as shown in Fig. 4. The slopes of the upstream channel and the downstream channel were 18 degrees and 7 degrees, respectively. A sediment bed of 1.9m long and 7cm deep was positioned from 2.8m to 4.7m upstream measured from the debouching point and soaked by the seepage flow. Sediment materials with mean diameter d_m =2.39mm, maximum diameter d_{max} = 11.2mm, $\tan\phi$ =0.7 and sediment density σ =2.65g/cm^3 were used. The particle size distribution of the sediment bed is shown in Fig. 5. Cylindrical pieces of 38 driftwood pieces (density of driftwood ρ_d =0.785g/cm^3) were positioned on the sediment bed at intervals of 10cm c/c along the

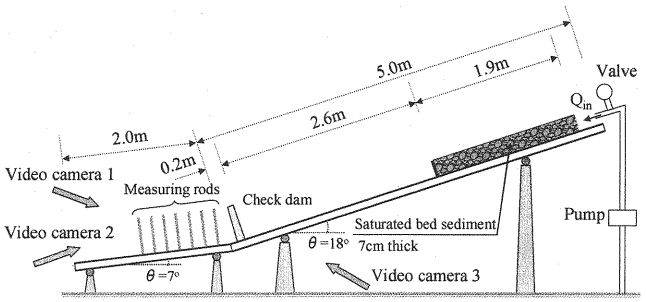

Fig. 4 Laboratory experimental flume setup

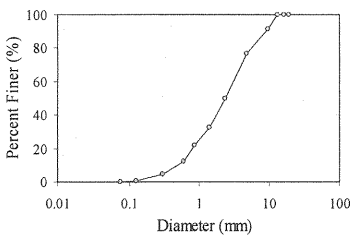

Fig. 5 Particle size distribution of sediment bed

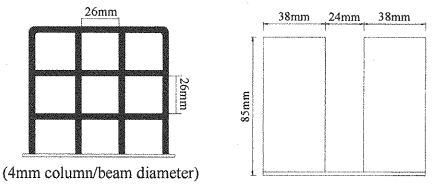

(a) Grid dam (b) Slit dam

Fig. 6 Detail of grid and slit type check dams

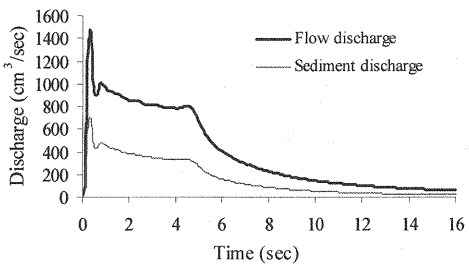

(a) Without driftwood

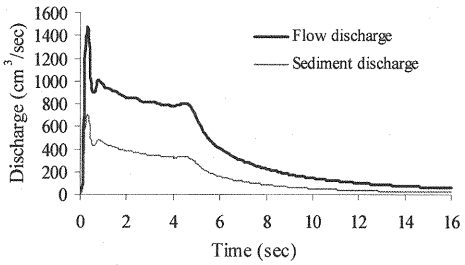

(b) With driftwood D_d=3mm and L_d=3.5cm

Fig. 7 Simulated discharge at 10cm upstream from debouching point, without check dam

downstream direction from 7.5cm downstream from the upstream end of the sediment bed in two columns 2cm apart. To investigate the effectiveness of check dams on the debris flow fan deposition, grid or slit type check dams were set at 20cm upstream from the debouching point. The details of check dams are shown in Fig. 6. Debris flow was produced by supplying a constant water discharge 270cm^3/sec for 10sec from the upstream end of the flume. The variations of the shapes and thicknesses of the deposit were measured by means of two video cameras, whereby the thickness of deposit was measured on the video image by reading out the elevations of the deposit surface using the gauging rods set on the downstream channel. The gauging rods were set at a rate of 10cm c/c intervals in both longitudinal and lateral positions.

RESULTS AND DISCUSSIONS

Numerical analyses were carried out to investigate the deposition of debris flow with driftwood on the fan. The parameters of the numerical simulation are as follows: the grid sizes Δx=5cm and Δy=1cm, the time interval

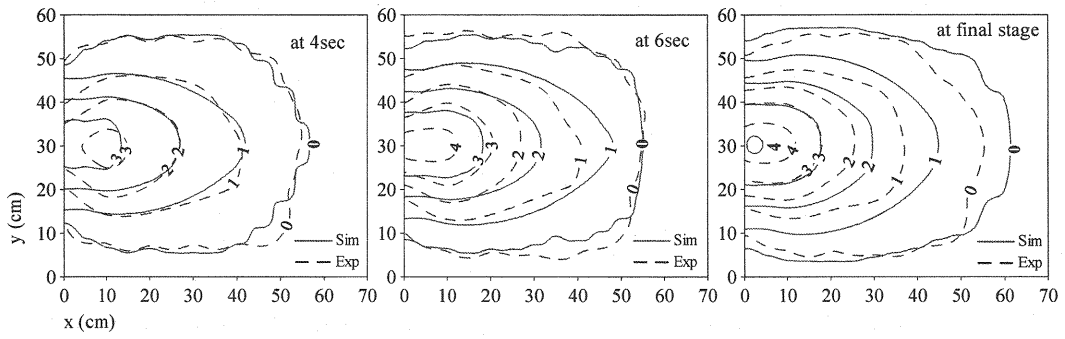

Fig. 8 Temporal changes of shapes and thicknesses of a debris flow fan, with driftwood D_d=3mm and L_d=3.5cm, without check dam

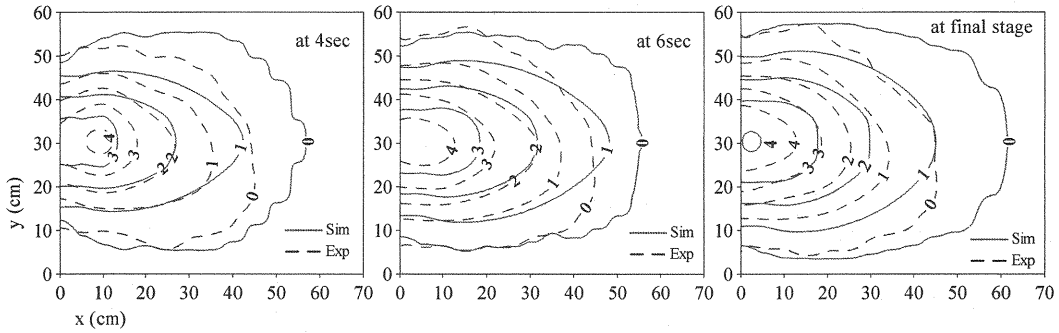

Fig. 9 Temporal changes of shapes and thicknesses of a debris flow fan, with driftwood D_d=3mm and L_d =4.5cm, without check dam

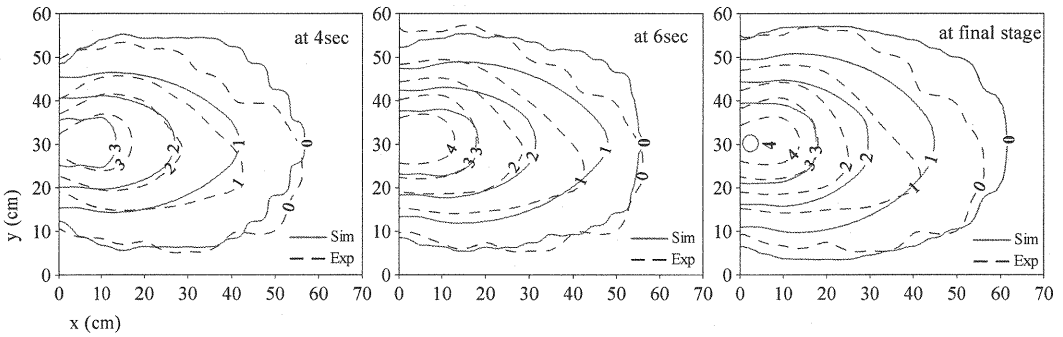

Fig. 10 Temporal changes of shapes and thicknesses of a debris flow fan, without driftwood and check dam

Δt = 0.001sec, ρ = 1.0g/cm^3, C_3= 0.48, g = 980cm/sec^2, n = 0.04, C_* =0.65, C_{Dx} =1.0, C_{Dy} =1.0, δ_e =0.0018, δ_d =0.045 (for upstream channel) and δ_d =1.0 (for downstream channel), C_M =1.0, μ_{kx} =0.3 and μ_{ky} =0.11. By using the same values of friction coefficients in x and y directions, it is difficult to get the same results as experimental. Thus, the different values of the friction coefficients in x and y directions are used to get good results with compared to the experimental results.

Driftwood as floating objects was considered and the initial movement of driftwood was evaluated with the flow depth and the respective velocity components of the fluid. Fig. 7 shows the simulated flow and sediment discharge at

10cm upstream from a debouching point of the flume. Figs. 8 and 9 show the simulated and experimental results of the temporal variations of the shapes and thicknesses (i.e., the flow depth plus the deposit thickness) in the process of a debris flow fan formation with driftwood D_d=3mm (D_d=diameter of the driftwood), L_d=3.5cm and D_d=3mm, L_d=4.5cm cases, respectively. The numbers on the contour lines indicate the thickness in centimeters measured from the surface of the downstream deposition channel. The simulated results were consistent with the experimental results. The results of the temporal variations of the shapes and thicknesses of a debris flow fan without driftwood case are shown in Fig. 10. By comparing the simulated results of the deposition of debris flow on the fan with and without driftwood cases, we found that the effect of driftwood in the deposition of debris flow on the fan was small, but the position and travel distance of the driftwood on the fan are very important for the evaluation of the risks of the hazards. The effect of driftwood in debris flow motion was evaluated by considering surface shear stress. There were some changes in the results because of the presence of driftwood and the driftwood sizes. However, findings showed the flow motion or fan deposition did not significantly change because of the presence of driftwood and the size.

The friction forces generated between the driftwood and bed surface in Eqs. 34 and 35 were considered only in the downstream channel to calculate the driftwood deposition in a debris flow fan. Based on the experimental investigations and numerical analyses, these friction forces were considered when the flow depth is less or equal to the sum of the depth of the submerged part of the driftwood and sediment particle diameter. The depth of the submerged part of the driftwood was calculated by equating the weight of the driftwood piece and the weight of fluid occupied by the volume of a piece of driftwood. The comparisons between the simulated and experimental positions and rotational angles of deposited driftwood in a debris flow fan are shown in Fig. 11. The dashed line in the figures indicates the debris flow fan area. The positions and the rotational angles of the pieces of driftwood in a group found experimentally were fairly well explained by the numerical simulation.

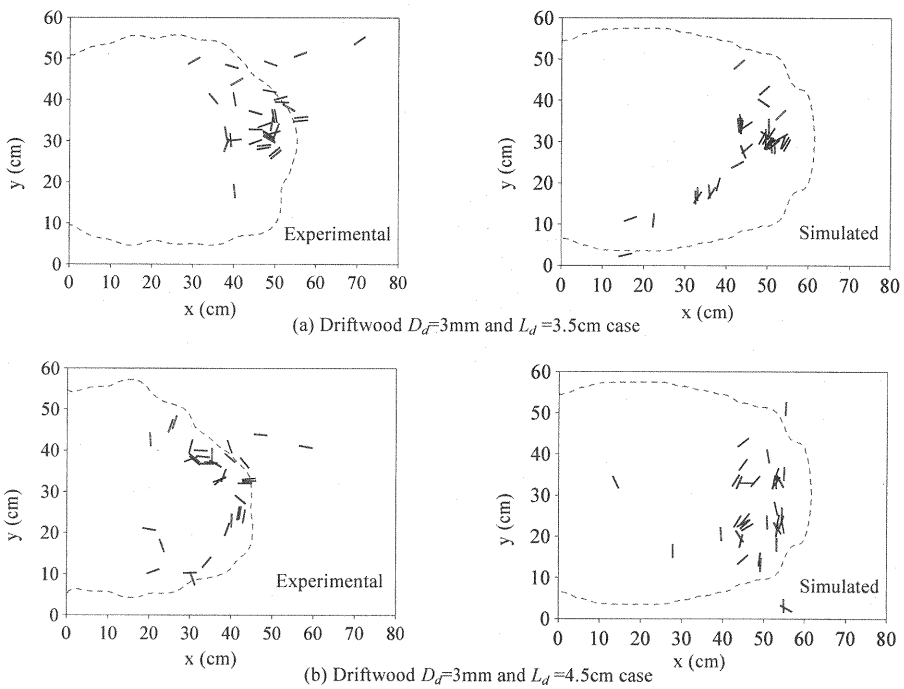

(a) Driftwood D_d=3mm and L_d =3.5cm case

(b) Driftwood D_d=3mm and L_d =4.5cm case

Fig. 11 Positions and rotational angles of deposited driftwood in a debris flow fan, with driftwood cases (a) D_d=3mm and L_d =3.5cm (b) D_d=3mm and L_d =4.5cm, without check dam

The effectiveness of check dams in a debris flow fan is also investigated through the numerical model and hydraulic experiments. The capturing process of debris flow and driftwood by check dam is used as Shrestha et al. (14). The sediment got deposited behind the check dam due to driftwood jamming. The temporal bed variation due to sediment deposition behind the check dam in a vertical direction was calculated by using the deposition velocity equation developed by Shrestha et al. (14) as follows:

$$i_{dep} = -(1-P_s)Q_{sed}/(C_*\Delta x) \tag{58}$$

where, i_{dep} = the deposition velocity equation upstream of check dam due to driftwood jamming; P_s = the sediment

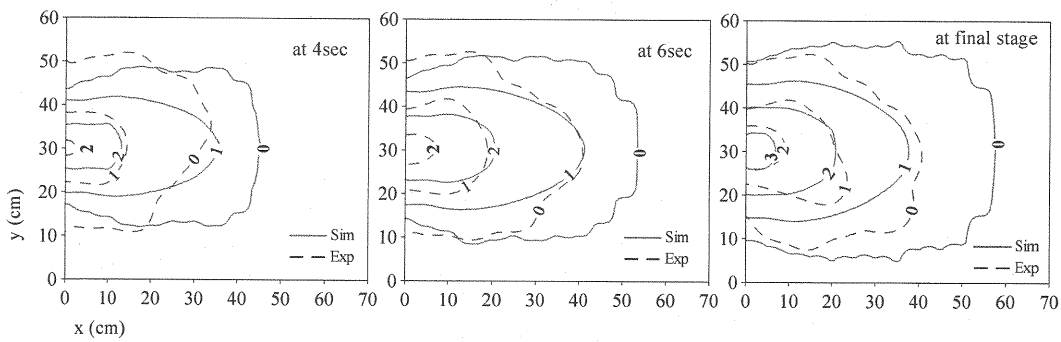

Fig. 12 Temporal changes of shapes and thicknesses of a debris flow fan, with driftwood D_d=3mm and L_d =3.5cm, and grid dam

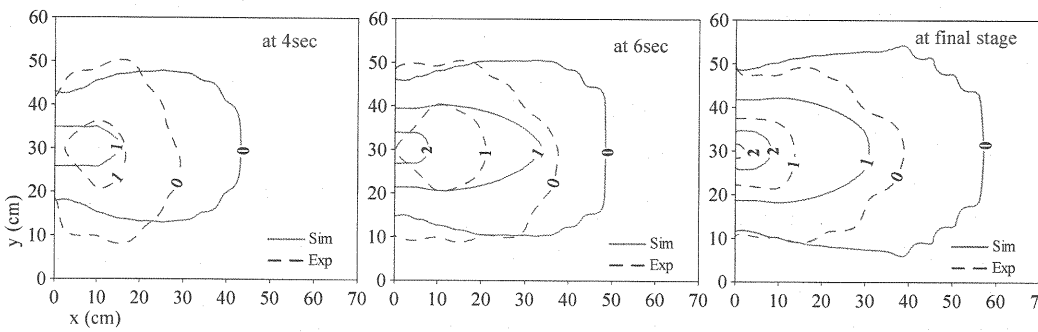

Fig.13 Temporal changes of shapes and thicknesses of a debris flow fan, with driftwood D_d=3mm and L_d =3.5cm, and slit dam case

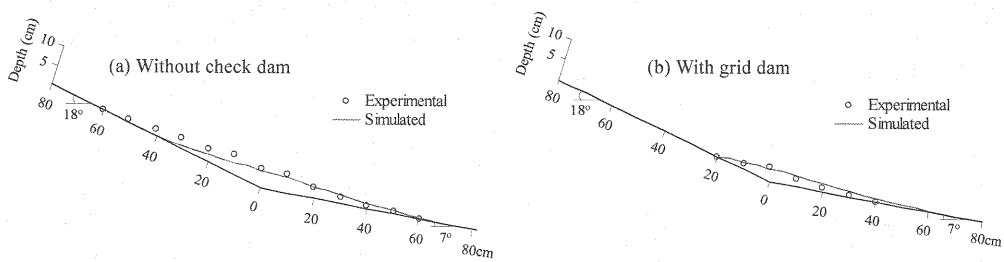

Fig. 14 The final stage longitudinal bed profile along center axis of debris flow fan, driftwood D_d=3mm and L_d =3.5cm case

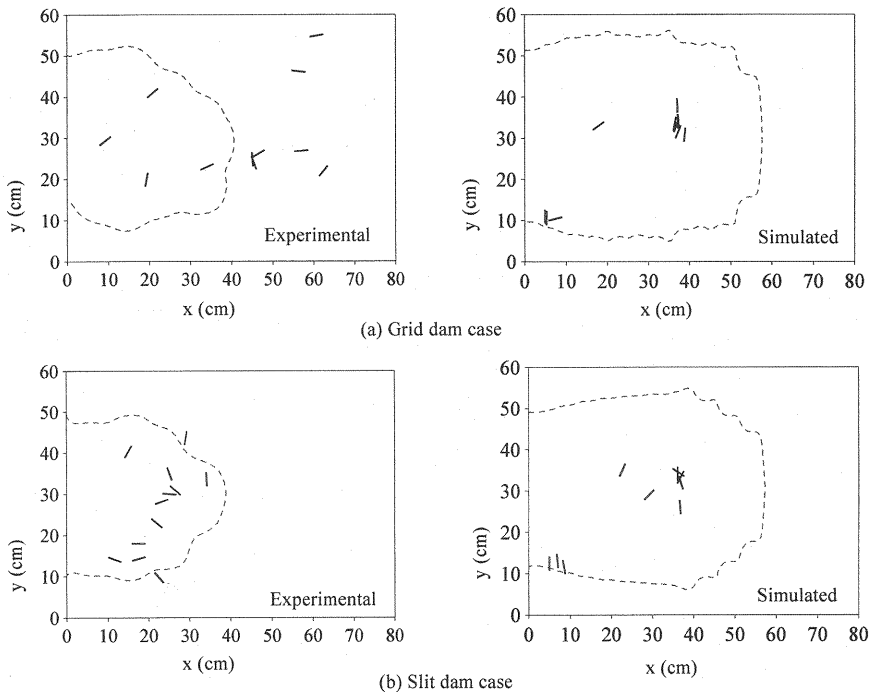

Fig. 15 Positions and rotational angles of deposited driftwood in a debris flow fan, with check dams and driftwood D_d=3mm and L_d =3.5cm

discharge passing rate through check dam (14); Q_{sed} = the sediment discharge per unit width; and Δx is the distance increment of calculating point.

Figs. 12 and 13 show the temporal variations of the shapes and thicknesses of a debris flow fan with grid dam and slit dam, respectively for the case of driftwood D_d=3mm, L_d=3.5cm. Some discrepancies were observed in the simulated and experimental fan deposition, which may have been due to some variations of sediment deposition behind the check dam in simulated and experimental results. Findings clearly reveal that the deposition areas and thicknesses in the cases of check dams are smaller than without check dam case. The reduction of deposition areas and thicknesses of fan deposition by check dams depends on the maximum particle size in the flow and open spaces of check dams, because the sediment deposition behind the check dam strongly varies on these parameters. Fig. 14 compares the final stage longitudinal bed profile along the center axis of a debris flow fan without check dam and with grid dam, in the case of driftwood D_d=3mm, L_d=3.5cm. The positions and the rotational angles of deposited driftwood in a debris flow fan with grid and slit type check dams are shown in Fig. 15. The amount of deposited driftwood decreased on the fan area due to driftwood jamming on the check dams.

CONCLUSIONS

The deposition of debris flows with driftwood on the fan was investigated by means of numerical simulations and flume experiments. The calculated results of the shapes and thicknesses of a debris flow fan and the positions and the rotational angles of deposited driftwood in a debris flow fan were found to be consistent with the experimental results. The driftwood deposition in a debris flow fan was calculated by considering the friction forces generated between the driftwood and the bed surface. The positions and the travel distance of deposited driftwood are very important in order

to reduce the risks of the hazards. Some discrepancy was found between calculated and experimental results of the driftwood positions, which may have been due to some variations in the calculated and experimental results of debris flow fan deposition. In this study, the motion of driftwood was restricted near the flow surface and no collisions between driftwood were considered. The rotational motion of the driftwood was also supposed to be restricted on the flow surface, and the rotation on the vertical plane was not considered. These limitations of the study may have also had an influence on calculation results of the driftwood positions. Therefore, further studies are necessary to consider such limitations. The effects of check dams in the debris flow fan formation were also investigated. By constructing check dams in the river basin, we can reduce the hazards in the downstream fan area. The proposed model can be used to investigate preventive measures of debris flow disasters with driftwood.

REFERENCES

1. Takahashi, T., Nakagawa, H., Harada, T. and Yamashiki, Y. : Routing debris flows with particle segregation, Journal of Hydraulic Engineering, Vol.118, No.11, ASCE, pp.1490-1507, 1992.
2. Tsai, Y. F. : A debris-flow simulation model for the evaluation of protection structures, Journal of Mountain Science, Vol.4, No.3, pp.193-202, 2007.
3. Shieh, C. L., Jan, C. D. and Tsai, Y. F. : A numerical simulation of debris flow and its application, Natural Hazards, Vol.13, pp.39-54, 1996.
4. Ghilardi, P., Natale, L. and Savi, F. : Modeling debris flow propagation and deposition, Physics and Chemistry of the Earth (C), Vol.26, No.9, pp.651-656, 2001.
5. Rickenmann, D., Laigle, D., McArdell, B. W. and Hubl, J. : Comparison of 2D debris-flow simulation models with field events, Computational Geosciences, Vol.10, pp.241-264, 2006.
6. Shrestha, B. B., Nakagawa, H., Kawaike, K., Baba, Y. and Zhang, H. : Numerical simulation on debris-flow with driftwood and its capturing due to jamming of driftwood on a grid dam, Annual Journal of Hydraulic Engineering, Vol.53, JSCE, pp.169-174, 2009.
7. Nakagawa, H., Takahashi, T. and Ikeguchi, M. : Behavior of driftwood and the process of its damming up, Journal of Hydroscience and Hydraulic Engineering, Vol.13, No.2, JSCE, pp.55-67, 1995.
8. Shimizu, Y. and Osada, K. : Numerical simulation on the driftwood behavior in open-channel flows by using distinct element method, Proceedings of 8th International Conference on Hydro-Science and Engineering, 2008.
9. Takahashi, T. : Debris flow: Mechanics, Prediction and Countermeasures, Proceedings and Monographs, Taylor & Francis/Balkema, pp.1-448, 2007.
10. Takahashi, T. : Debris flow, Monograph Series of IAHR, Balkema, pp.1-165, 1991.
11. Nakagawa, H., Takahashi, T., Satofuka, Y., and Kawaike, K. : Numerical simulation of sediment disasters caused by heavy rainfall in Camuri Grande basin, Venezuela 1999, Proceedings of the 3rd Conference on Debris-Flow Hazards Mitigation: Mechanics, Prediction, and Assessment, pp.671-682, 2003.
12. Nakagawa, H. : Study on risk evaluation of flood and sediment inundation disaster, Doctoral Thesis, Kyoto University, 1989 (in Japanese).
13. Nakagawa, H., Takahashi, T. and Ikeguchi, M. : Numerical simulation of drift wood behavior, the Annuals of the Disaster Prevention Research Institute, Kyoto University, No.35 B-2, pp.249-266, 1992 (in Japanese).
14. Shrestha, B. B., Nakagawa, H., Kawaike, K., Baba, Y. and Zhang, H. : Capturing process of debris flow with driftwood by an open type check dam, the Annuals of the Disaster Prevention Research Institute, Kyoto University, No.52 B, pp.697-715, 2009.

APPENDIX – NOTATION

The following symbols are used in this paper:

a_i = experimental constant;

a_0 = constant value defined as 1/9.025;

A = area of the flow surface defined by $\Delta x \Delta y$;

A_{kx}, A_{ky} = respective projected areas of the submerged part of the driftwood in x and y directions;

C = sediment concentration in the flow;

C_{dl} = $0.4C_*$;

C_{Dx}, C_{Dy} = drag coefficients in x and y directions;

C_M = virtual mass coefficient;

C_3 = limitative sediment concentration defined as 0.48;

C_* = sediment concentration in the bed;

C_∞ = equilibrium sediment concentration;

d_m = mean diameter of sediment;

$d_{\max}$ = maximum diameter of sediment;

D_d = diameter of the driftwood piece;

erf, erf^{-1} = error function and its inverse function;

F_{fx}, F_{fy} = friction forces in x and y directions;

Fr = Froude number;

g = acceleration due to gravity;

h = flow depth;

h_l = thickness of the particle mixture layer in an immature debris flow;

h_w = depth of submerged part of driftwood in the fluid;

H_k = flow level at centroid position of the driftwood;

i_b = erosion/deposition velocity;

i_{dep} = deposition velocity behind check dam due to driftwood jamming;

I = moment of inertia around the centroid of the driftwood;

K_x, K_y = longitudinal and transverse diffusion coefficients;

L_d = length of the driftwood piece;

m = mass of the fluid occupied by volume of a piece of driftwood;

m_k = mass of the driftwood;

M = flow discharge per unit width in x direction;

n = Manning's coefficient;

N = flow discharge per unit width in y direction;

N_t = number of total pieces of driftwood in area A;

P_s = sediment passing rate through check dam;

Q_{sed} = sediment discharge per unit width;

r = radius of driftwood piece;

R_{*x} = $u_* h/\upsilon_0$;

R_{*y} = $v_* h/\upsilon_0$;

u, v = velocity components of the flow in x and y directions;

u_k, v_k = respective driftwood velocity components in x and y directions;

u_l, v_l = velocity components of the flow in x and y directions at the thickness of the particle mixture layer in an immature debris flow;

u_s, v_s = surface velocity components of debris flow in x and y directions;

u_*, v_* = friction velocity components in x and y directions;

U_k, V_k = respective local velocity components of the fluid in x and y directions;

W_k = relative velocity of the fluid with respect to the driftwood, i.e., $W_k = \sqrt{(u_k - U_k)^2 + (v_k - V_k)^2}$;

X_k, Y_k = position of the centroid of the driftwood;

z_b = erosion or deposition thickness of the bed measured from the original bed surface elevation;

α_i = collisions angle of the particles;

α_1 = angle between the depth of submerged part of driftwood up to center point of the driftwood diameter from the flow surface and the radius of driftwood piece with the flow surface;

α', β' = random variables uniformly distributed in the range (0,1);

β = momentum correction factor;

γ = $(\omega_p - \overline{\omega})/\sigma_w$;

δ_d = deposition coefficient;

δ_e = erosion coefficient;

Δt = time interval of the calculation;

Δx, Δy = grid sizes of the finite difference equations;

ΔX_k, ΔY_k = fluctuation components of the driftwood position in x and y directions;

ρ = density of the water;

ρ_d = density of driftwood piece;

ρ_T = mixture density of the fluid;

σ = density of the sediment particle;

σ_w = standard deviation of the rotational motion of the driftwood;

ϕ = internal friction angle of the sediment;

θ_{bx0}, θ_{by0} = slope of the original bed surface in x and y directions;

θ_k = rotational angle of the piece of driftwood;

θ_w = water surface slope;

θ_x, θ_y = slope of the bed surface in x and y directions;

κ = Karman constant;

ς = constant to describe the mixing length;

λ = linear concentrations;

τ_{bx}, τ_{by} = bottom shear stresses in x and y direction;

τ_{sx}, τ_{sy} = shear stresses at the flow surface in x and y directions;

τ_*, τ_{*c} = non-dimensional shear stress and non-dimensional critical shear stress;

υ_0 = kinematic viscosity of plain water;

μ_{kx}, μ_{ky} = kinetic friction coefficients in x and y directions;

$\overline{\omega}$ = mean angular velocity of the driftwood;

ω_d = angular velocity of the piece of driftwood obtained deterministically; and

ω_p = fluctuation of the angular velocity of the driftwood evaluated stochastically.

(Received Jul, 09, 2010 ; revised Feb, 24, 2011)